Available online at www.sciencedirect.com
SCIENCE DIRECT®
C. R. Mecanique 334 (2006) 341–346
COMPTES RENDUS MECANIQUE
http://france.elsevier.com/direct/CRAS2B/

Large-amplitude internal solitary waves in a two-fluid model

Philippe Guyenne

Department of Mathematical Sciences, 501 Ewing Hall, University of Delaware, Newark, DE 19716-2553, USA

Received 10 April 2006; accepted 25 April 2006

Available online 6 June 2006

Presented by Gérard Iooss

Abstract

We compute solitary wave solutions of a Hamiltonian model for large-amplitude long internal waves in a two-layer stratification. Computations are performed for values of the density and depth ratios close to oceanic conditions, and comparisons are made with solutions of both weakly and fully nonlinear models. It is shown that characteristic features of highly nonlinear solitary waves such as broadening are reproduced well by the present model. ***To cite this article: Ph. Guyenne, C. R. Mecanique 334 (2006).***

Résumé

Ondes solitaires internes de grande amplitude dans un modèle à deux fluides. Nous calculons numériquement des solutions en ondes solitaires d'un modèle hamiltonien décrivant les ondes internes longues de grande amplitude dans un milieu stratifié à deux couches. Ces solutions numériques sont calculées pour des valeurs de rapports de densité et de profondeur proches des conditions océaniques, et sont comparées avec les solutions de modèles faiblement et pleinement non-linéaires. Les résultats montrent que le modèle reproduit bien les caractéristiques des ondes solitaires fortement non-linéaires telles que le phénomène d'élargissement. ***Pour citer cet article : Ph. Guyenne, C. R. Mecanique 334 (2006).***

Keywords: Fluid mechanics; Internal waves; Solitary waves; Hamiltonian systems

Mots-clés : Mécanique des fluides ; Ondes internes ; Ondes solitaires ; Systèmes hamiltoniens

1. Introduction

Internal solitary waves are ubiquitous in oceans, fjords and lakes. They are frequently observed in coastal regions where strong tides and stratification occur over variable topography. They often exhibit very large amplitudes. General properties of such waves have been described in detail; see, e.g., the review [1].

Models based on the full Euler equations have greatly contributed to our understanding of nonlinear internal wave properties [2–7]. However, numerical simulations based on these models are usually computationally expensive. Recently long wave models, combining both relative simplicity and full nonlinearity, have been developed and have been found to compare well with experiments [8–10].

E-mail address: guyenne@math.udel.edu (Ph. Guyenne).

1631-0721/$ – see front matter
doi:10.1016/j.crme.2006.05.001

Motivated by these works, Craig, Guyenne and Kalisch [11,12] recently derived a Hamiltonian model for large-amplitude long internal waves in a two-layer configuration. To our knowledge, solutions of this model have never been investigated before. We provide here the first numerical evidence of solitary wave solutions. These are computed for parameters close to oceanic conditions, and are compared with solutions of both weakly and fully nonlinear models.

2. Hamiltonian two-fluid model

We consider two-dimensional wave motion of an interface between two immiscible ideal fluids of finite depth, described by the Hamiltonian system [11,12]

$$\partial_t \eta = -\partial_x \delta_u \mathbb{H}, \qquad \partial_t u = -\partial_x \delta_\eta \mathbb{H} \tag{1}$$

with Hamiltonian

$$\mathbb{H} = \frac{1}{2}\int_{\mathbb{R}} \left[R_0(\eta)u^2 + g(\rho-\rho_1)\eta^2 + R_1(\eta)(\partial_x u)^2 + \big(\partial_x R_2(\eta)\big)\partial_x\big(u^2\big) + R_3(\eta)(\partial_x\eta)^2 u^2\right] \mathrm{d}x \tag{2}$$

where $\eta(x,t)$ is the interface displacement, $u(x,t)$ is the jump of horizontal velocity across the interface, and g is the acceleration due to gravity. The lower fluid is of density ρ and depth h, and the lighter, upper fluid is of density ρ_1 and depth h_1. Surface tension effects are neglected and rigid lid boundary conditions are imposed. Here $R_0(\eta)$, $R_1(\eta)$, $\partial_x R_2(\eta)$ and $R_3(\eta)$ are rational functions of η. Their (cumbersome) expressions are not shown here for convenience and the reader is referred to [11,12] for further details.

This model can be formally derived from the full Euler equations for two-layer potential flows. One assumes that the typical wavelength of the internal waves is long as compared to the depths of the fluids, but no smallness assumption on wave amplitude is made. A counterpart to (1) for small wave amplitudes is given by the Kaup–Boussinesq (KB) equations, which are fully integrable and which admit solitary wave solutions of the form

$$\eta(x,t) = \frac{c}{\beta}u(x,t) - \frac{\gamma}{2\beta}u(x,t)^2, \quad u(x,t) = 2\frac{\sqrt{\alpha\beta}}{\gamma}\frac{(\frac{c^2}{\alpha\beta}-1)}{\cosh(\sqrt{\frac{\alpha}{\delta}(\frac{c^2}{\alpha\beta}-1)}(x-ct)) + \frac{c}{\sqrt{\alpha\beta}}} \tag{3}$$

where

$$\alpha = \frac{hh_1}{\rho_1 h + \rho h_1}, \quad \beta = g(\rho-\rho_1), \quad \delta = \frac{1}{3}\frac{(hh_1)^2(\rho_1 h_1 + \rho h)}{(\rho_1 h + \rho h_1)^2}, \quad \gamma = \frac{\rho h_1^2 - \rho_1 h^2}{(\rho_1 h + \rho h_1)^2} \tag{4}$$

and c denotes the wave speed.

3. Solitary wave solutions and numerical scheme

We look for solutions of (1) which are stationary in a reference frame moving at constant speed c and which decay very fast at infinity. These correspond to fixed points of $\delta(\mathbb{H} - cI)$, where $I = \int_{\mathbb{R}} \eta u \,\mathrm{d}x$ is the momentum of the system. We thus need to solve the following system of nonlinear, ordinary differential equations

$$\begin{aligned} 0 &= -c\eta + R_0 u - (R_1 u')' - (R_2)'' u + R_3(\eta')^2 u \\ 0 &= -cu + \frac{1}{2}(\partial_\eta R_0)u^2 + g(\rho-\rho_1)\eta + \frac{1}{2}(\partial_\eta R_1)(u')^2 - \frac{1}{2}(\partial_\eta R_2)\big(u^2\big)'' + \frac{1}{2}(\partial_\eta R_3)(\eta')^2 u^2 - \big(R_3\eta' u^2\big)' \end{aligned} \tag{5}$$

where the symbol $'$ stands for differentiation with respect to x. Note that $\partial_\eta R_2$ in (5) is related to $\partial_x R_2$ through the chain rule $\partial_x R_2 = \partial_\eta R_2\, \partial_x \eta$.

System (5) can be easily discretized using a pseudospectral method and assuming periodic boundary conditions in x. Both η and u are expanded in truncated Fourier series with the same number of modes N. All operations are performed using the fast Fourier transform, which yields high accuracy at relatively low cost. We solve the resulting discretized system by an iterative procedure (Newton–Raphson's method), and the bifurcation parameter in the problem is the wave speed c. Because small-amplitude waves of the KB equations are close approximations to those of (1) in the weakly nonlinear regime, we use the KB solutions (3) as the initial guess in the iterative procedure, to find solitary wave solutions of (1). We then gradually increase the parameter c (thus increasing the wave amplitude) and repeat the procedure, using smaller-amplitude solutions as an initial guess to compute higher-amplitude solutions.

4. Numerical results

Computations have been performed with a discretization $N = 1024$, for a domain of length $L/h = 50$. The domain is specified long enough to ensure that the tails of the solitary waves are rapidly decaying at its ends and that periodicity has no significant effect on the solutions. As determined by the initial guess (3), we look for solitary waves moving at speeds $c^2 > c_0^2 = \alpha\beta = ghh_1(\rho - \rho_1)/(\rho_1 h + \rho h_1)$ where c_0 denotes the linear wave speed for two-layer flows. Fig. 1 shows the computed wave profiles for $h_1/h = 1/3$ and $\rho/\rho_1 = 0.997$; the solitary waves being of depression in this case. This regime of parameters was chosen because it is representative of situations close to oceanic conditions [2]. The linear wave speed in this configuration is $c_0/\sqrt{gh} = 0.0274$ (or $c_0/\sqrt{gh_1} = 0.0475$). For comparison, solitary

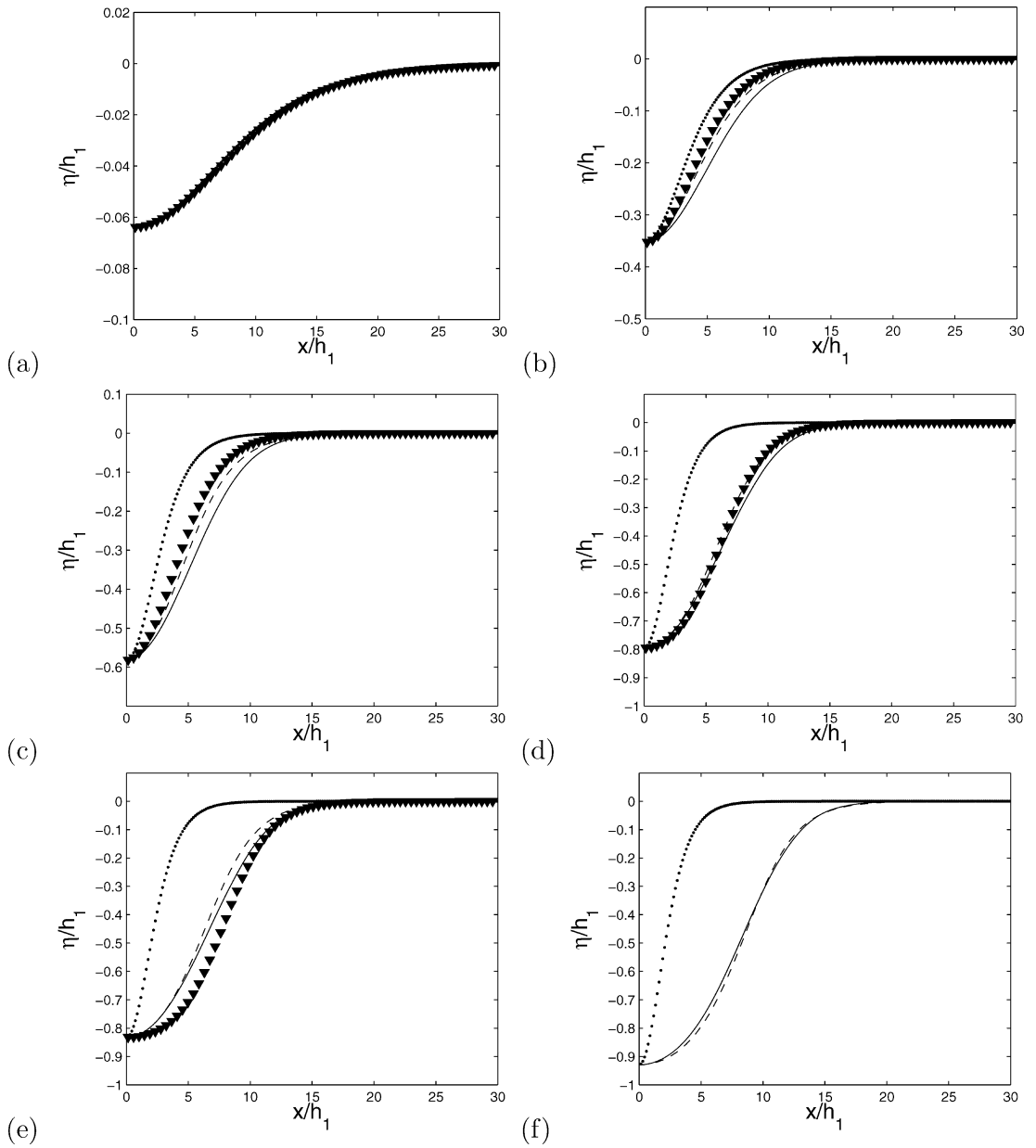

Fig. 1. Comparison of wave profiles η for the KdV equation (dots), Gardner equation (triangles), fully nonlinear model of Grue et al. [5] (dashed line) and present model (solid line). The parameters are $h_1/h = 1/3$ and $\rho_1/\rho = 0.997$. The different plots correspond to amplitudes (a) $H/h_1 = 0.064$, (b) $H/h_1 = 0.353$, (c) $H/h_1 = 0.582$, (d) $H/h_1 = 0.795$, (e) $H/h_1 = 0.833$, (f) $H/h_1 = 0.929$.

wave solutions of the Korteweg–de Vries (KdV) and Gardner equations [13,14] as well as those computed by the fully nonlinear model of Grue et al. [5], with matching amplitudes, are also shown in the figure. The model of Grue et al. [5] solves the full equations for two-layer flows using a boundary integral method. The KdV equation has a family of well-known 'sech^2' solitary wave solutions. For the Gardner equation (also known as the extended KdV equation), the solitary waves (also called kink-antikink solutions) are of the form

$$\eta(x,t) = -\frac{\alpha}{\alpha_1}\frac{\nu}{2}\left[\tanh\left(\frac{x-ct}{\Delta}+\delta\right) - \tanh\left(\frac{x-ct}{\Delta}-\delta\right)\right] \tag{6}$$

where

$$\alpha = \frac{3c_1(h_1-h)}{2hh_1}, \quad \alpha_1 = \frac{3c_1}{h^2h_1^2}\left[\frac{7}{8}(h-h_1)^2 - \frac{h^3+h_1^3}{h+h_1}\right], \quad c_1^2 = \frac{ghh_1(\rho-\rho_1)}{\rho(h+h_1)} \tag{7}$$

$$\Delta^2 = -\frac{24\alpha_1\beta}{\alpha^2\nu^2}, \quad \beta = \frac{c_1hh_1}{6}, \quad c = c_1 - \frac{\alpha^2\nu^2}{6\alpha_1}, \quad \delta = \frac{1}{4}\ln\left(\frac{1+\nu}{1-\nu}\right) \tag{8}$$

and ν is a nonlinearity parameter with values $0 < \nu < 1$. Solitary waves of the Gardner equation are broader than their KdV analogues, and they become more box shaped with flat crests (table-top solutions) as the amplitude increases toward the limit $\alpha/\alpha_1 = 0.857h_1$ (hereafter we define the wave amplitude as $H = |\eta|_{\max}$).

As expected, for small amplitudes, the KdV wave profiles are close to those of (1) but the latter become significantly broader as the amplitude increases. Broad internal solitary waves have also been observed by other authors, e.g., [15–17]. We see in Fig. 1 that the 'computed' profiles (i.e., of model (1)) are also broader than the Gardner and fully nonlinear profiles for amplitudes up to $H/h_1 \simeq 0.795$; the fully nonlinear solutions lying between the Gardner and computed ones. For $H/h_1 \simeq 0.795$, the computed, Gardner and fully nonlinear wave shapes almost coincide, especially in the lower part around the wave crest. For higher amplitudes, as $\nu \to 1$, the picture is reversed; the Gardner solitary waves flatten and become broader than the computed and fully nonlinear waves. Such differences in wave shapes are further quantified in Fig. 2 which compares the width W (at mid-amplitude $H/2$) for the four types of solitary waves. It can be clearly seen that the width for the KdV solution continuously decreases as H grows, while that for the other three solutions increases past $H/h_1 \simeq 0.45$. Although the width of the Gardner solitary wave is smaller than those of the computed and fully nonlinear waves for most amplitudes, it increases faster as H approaches $0.857h_1$ due to the flattening process.

Despite these noticeable differences in wave profiles, we see in Fig. 3 that the speeds of the computed, Gardner and fully nonlinear solitary waves are quite close over almost the entire range of amplitudes considered. In fact, the curves for the computed and fully nonlinear solutions are almost indistinguishable, while that for the Gardner solution

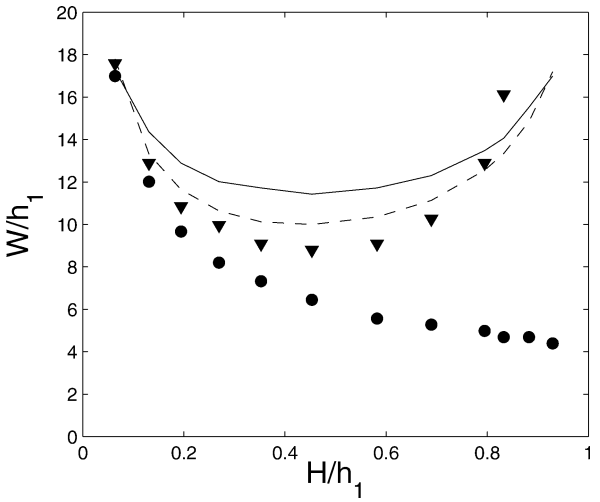

Fig. 2. Comparison of solitary wave widths W (at mid-amplitude $H/2$) for the KdV equation (dots), Gardner equation (triangles), fully nonlinear model of Grue et al. [5] (dashed line) and present model (solid line).

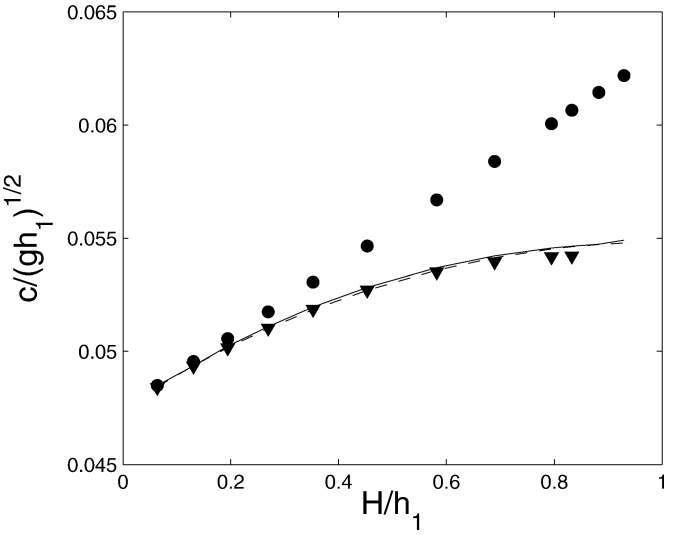

Fig. 3. Comparison of wave speeds c for the KdV equation (dots), Gardner equation (triangles), fully nonlinear model of Grue et al. [5] (dashed line) and present model (solid line).

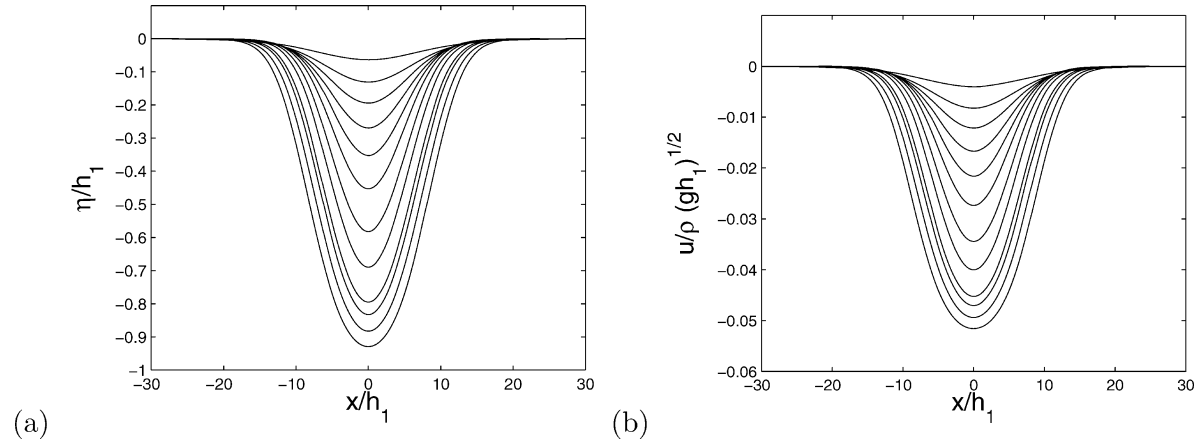

Fig. 4. Sequence of computed profiles of (a) η and (b) u. The different curves correspond to amplitudes $H/h_1 = 0.064, 0.131, 0.194, 0.269, 0.353, 0.453, 0.582, 0.689, 0.795, 0.833, 0.882, 0.929$.

lies slightly below at large amplitudes. Their speeds exhibit a similar slow growth which seems to reach a maximum around $c/\sqrt{gh_1} \simeq 0.055$ (i.e., the conjugate flow limit; see below). This contrasts with the speed of the KdV solution which grows linearly with the amplitude. It should be pointed out that the range of large amplitudes we are considering here (i.e., $H/h_1 \simeq 0.795$ or so) is certainly beyond the regime of validity of both the KdV and Gardner equations. Nonetheless, the similarities that we observe between the computed, Gardner and fully nonlinear solutions suggest that the present model reproduces well characteristic features of large-amplitude internal solitary waves.

As shown in Fig. 1(f), we were able to compute solutions of (1) for amplitudes higher than $0.857h_1$, which corresponds to the maximum amplitude for Gardner solitary waves in the present configuration. This explains why the comparison with the Gardner solution is not shown in the figure. The maximum wave amplitude and speed that our computations could achieve are $H/h_1 = 0.929$ and $c/\sqrt{gh_1} = 0.0549$, which are close to the limiting amplitude and speed for conjugate flows as given by

$$H_{\max} = \frac{h\sqrt{\rho_1} - h_1\sqrt{\rho}}{\sqrt{\rho} + \sqrt{\rho_1}} = 0.998h_1, \qquad c_{\max} = \frac{\sqrt{g(h+h_1)(\rho-\rho_1)}}{\sqrt{\rho} + \sqrt{\rho_1}} = 0.0548\sqrt{gh_1} \tag{9}$$

Evans and Ford [2] computed extremal forms of internal solitary waves very close to this limit for $h_1/h = 1/3$ and $\rho/\rho_1 = 0.997$, using an integral equation model based on the full Euler equations. Finally, Fig. 4(a) presents a sequence of wave profiles, solutions of (1), which clearly shows that the width of the computed solitary waves continuously grows with the amplitude. A similar behavior is observed for the profile of u in Fig. 4(b).

In conclusion, solitary wave solutions of system (1) have been computed in a parameter regime close to oceanic conditions. The solitary waves are found to be significantly broader and slower than their KdV analogues; their width increasing with the amplitude. The present model compares better than the Gardner equation with the fully nonlinear model of Grue et al. [5] for large amplitudes. We were able to compute solutions for amplitudes up to $H/h_1 = 0.929$, which is close to the conjugate flow limit. It would be worthwhile to compare with experiments in the future. Finally, the present study is focused on solitary wave solutions of (1), but problems of time evolution can also be considered.

Acknowledgements

The author would like to thank W. Craig and H. Kalisch for encouraging and helpful discussions. Computations of fully nonlinear solitary waves have been performed using The Internal Wave Program, developed by Per-Olav Rusås at the University of Oslo, and documented in Grue et al. [5].

References

[1] K.R. Helfrich, W.K. Melville, Long nonlinear internal waves, Annu. Rev. Fluid Mech. 38 (2006) 395–425.
[2] W.A.B. Evans, M.J. Ford, An integral equation approach to internal (2-layer) solitary waves, Phys. Fluids 8 (1996) 2032–2047.
[3] O. Laget, F. Dias, Numerical computation of capillary-gravity interfacial solitary waves, J. Fluid Mech. 349 (1997) 221–251.
[4] H. Michallet, E. Barthélémy, Experimental study of interfacial solitary waves, J. Fluid Mech. 366 (1998) 159–177.
[5] J. Grue, A. Jensen, P.-O. Rusås, J.K. Sveen, Properties of large-amplitude internal waves, J. Fluid Mech. 380 (1999) 257–278.
[6] P.-O. Rusås, J. Grue, Solitary waves and conjugate flows in a three-layer fluid, Eur. J. Mech. B/Fluids 21 (2002) 185–206.
[7] F. Dias, J.-M. Vanden-Broeck, On internal fronts, J. Fluid Mech. 479 (2003) 145–154.
[8] W. Choi, R. Camassa, Fully nonlinear internal waves in a two-fluid system, J. Fluid Mech. 396 (1999) 1–36.
[9] L.A. Ostrovsky, J. Grue, Evolution equations for strongly nonlinear internal waves, Phys. Fluids 15 (2003) 2934–2948.
[10] R. Camassa, W. Choi, H. Michallet, P.-O. Rusås, J.K. Sveen, On the realm of validity of strongly nonlinear asymptotic approximations for internal waves, J. Fluid Mech. 549 (2006) 1–23.
[11] W. Craig, P. Guyenne, H. Kalisch, A new model for large amplitude long internal waves, C. R. Mecanique 332 (2004) 525–530.
[12] W. Craig, P. Guyenne, H. Kalisch, Hamiltonian long wave expansions for free surfaces and interfaces, Comm. Pure Appl. Math. 58 (2005) 1587–1641.
[13] T.P. Stanton, L.A. Ostrovsky, Observations of highly nonlinear internal solitons over the continental shelf, Geophys. Res. Lett. 25 (1998) 2696–2698.
[14] R. Grimshaw, D. Pelinovsky, E. Pelinovsky, A. Slunyaev, Generation of large-amplitude solitons in the extended Korteweg–de Vries equation, Chaos 12 (2002) 1070–1076.
[15] R. Grimshaw, D. Pullin, Extreme interfacial waves, Phys. Fluids 29 (1986) 2802–2807.
[16] R.E.L. Turner, J.-M. Vanden-Broeck, Broadening of interfacial solitary waves, Phys. Fluids 31 (1988) 2486–2490.
[17] K.G. Lamb, B. Wan, Conjugate flows and flat solitary waves for a continuously stratified fluid, Phys. Fluids 10 (1998) 2061–2079.